Published in final edited form as:
Dev Cell. 2012 November 13; 23(5): 925–938. doi:10.1016/j.devcel.2012.09.019.

Arl13b in primary cilia regulates the migration and placement of interneurons in the developing cerebral cortex

Holden Higginbotham[1], **Tae-Yeon Eom**[1], **Laura E. Mariani**[2,3], **Amelia Bachleda**[1], **Vladimir Gukassyan**[1], **Joshua Hirt**[1], **Corey Cusack**[1], **Cary Lai**[4], **Tamara Caspary**[3,^], and **E. S. Anton**[1,^]

[1]UNC Neuroscience Center and the Department of Cell Biology and Physiology, University of North Carolina School of Medicine, Chapel Hill, NC 27599

[2]Neurosciences Graduate Program

[3]Department of Human Genetics, Emory University School of Medicine, Atlanta, GA 30322

[4]Gill Center for Biomolecular Science, Indiana University, Bloomington, IN 47405

Abstract

Coordinated migration and placement of interneurons and projection neurons lead to functional connectivity in the cerebral cortex; defective neuronal migration and the resultant connectivity changes underlie the cognitive defects in a spectrum of neurological disorders. Here we show that primary cilia play a guiding role in the migration and placement of postmitotic interneurons in the developing cerebral cortex, and that this process requires the ciliary protein, Arl13b. Through live imaging of interneuronal cilia we show migrating interneurons display highly dynamic primary cilia and we correlate cilia dynamics with the interneuron's migratory state. We demonstrate that the guidance cue receptors essential for interneuronal migration localize to interneuronal primary cilia, but their concentration and dynamics are altered in the absence of Arl13b. Expression of Arl13b variants known to cause Joubert syndrome induce defective interneuronal migration, suggesting that defects in cilia-dependent interneuron migration may underlie the neurological defects in Joubert syndrome patients.

Keywords

Ciliopathies; microfluidics; Arl13b; Joubert Syndrome

INTRODUCTION

The appropriate placement of neurons in the cerebral cortex, achieved through a coordinated process of oriented neuronal migration, is critical for the emergence of functional neural circuitry underlying higher order brain functions. Neuronal migration enables distinct classes of neurons to navigate from their sites of birth in the progenitor zones to their final

[^]**Correspondence to:** E. S. Anton, UNC Neuroscience Center and the Department of Cell Biology and Physiology, The University of North Carolina School of Medicine, Chapel Hill, NC 27599, anton@med.unc.edu, PHONE: 919-843-6114, FAX: 919-966-1844 Tamara Caspary, Dept. Of Human Genetics, Emory University School of Medicine, Atlanta, GA 30322, tcaspar@emory.edu, PHONE: 404-727-9862, FAX: 404-727-3949.

laminar and areal destinations within the cerebral cortex (Ayala et al., 2007; Marin et al., 2010; Rakic et al., 1972). An efficient, selective intracellular response to extracellular signaling cues is fundamental in coordinating these diverse migratory processes. Primary cilia are found on cortical neuronal progenitors and neurons and may play a guiding role in the construction of the cerebral cortex (Arellano et al., 2012; Bishop et al., 2007; Han and Alvarez-Buylla, 2010; Handel et al., 1999; Lee and Gleeson, 2011; Wilson et al., 2012). The potential significance of cilia function for cortical development and function is evident in various developmental brain disorders such as Joubert, Meckel-Gruber, Orofaciodigital, and Bardet-Biedl syndromes (commonly referred to as ciliopathies), where disrupted cilia function and the resultant changes in cortical formation are thought to underlie the cognitive deficits associated with these syndromes (Hildebrandt et al., 2011).

The primary cilium may play a role in the progression of cortical neuronal development. The basal bodies, which reside at the base of the cilium and are required for its formation, are located in the leading process of migrating neurons and are hypothesized to be involved in leading process stability and nuclear translocation (Metin et al., 2008; Higginbotham and Gleeson, 2007; Solecki et al., 2004). Recent studies using ciliogenic mutants indicate that ependymal cilia and primary cilia activity in the neurogenic zones of the developing cortex are required for the appropriate proliferation of progenitors and generation of neurons (Amador-Arjona et al., 2011; Besse et al., 2011; Breunig et al., 2008; Willaredt et al., 2008). Although these studies demonstrate the importance of cilia activity in progenitor dynamics, little is known about how neuronal cilia may influence the migration and differentiation of distinct classes of neurons during corticogenesis. We therefore aimed to identify the essential functions of primary cilia in neuronal migration and differentiation in the developing cerebral cortex.

To study the role of cilia in neuronal migration and differentiation, we used a mouse genetic model in which cilia function can be impaired in a temporal and neuronal type-specific manner. Arl13b, a small GTPase of the Arf/Arl family, is specifically localized to cilia (Caspary et al., 2007). Deletion of Arl13b in mouse results in impaired cilia, which lose their ability to function as conveyors of critical extracellular signals (Caspary et al., 2007). In humans, mutations in ARL13B result in Joubert syndrome (Cantagrel et al., 2008). Thus, neuronal type and developmental stage-specific genetic manipulation of Arl13b function provides a model to disrupt the primary function of cilia in distinct classes of neurons during corticogenesis and evaluate how this affects neuronal migration, placement, and the formation of cerebral cortex. Towards this goal, we conditionally disrupted primary cilia function in postmitotic projection neurons and interneurons and define a role for primary cilia activity in the oriented migration and placement of interneurons.

RESULTS

Conditional deletion of Arl13b in the developing cortical neurons

Arl13b is expressed in the primary cilia of post-mitotic cortical neurons during embryonic and post-natal development (Figure S1 A-H). We conditionally ablated Arl13b in distinct subsets of post-mitotic neurons of the developing cerebral cortex using the Cre-Lox recombination system (Su et al, 2012). We specifically targeted the two major populations of cortical neurons using the Nex-Cre or the Dlx5/6-Cre-IRES-EGFP (Dlx5/6-CIE) transgenic lines, which express Cre in postmitotic, radially migrating projection neurons or in postmitotic, tangentially migrating, subcortically-derived interneurons, respectively, and confirmed cell type specific deletion of Arl13b (Figure S1 I-P) (Goebbels et al., 2006; Stenman et al., 2003; Wu et al., 2005). We also incorporated a Tau-Lox-STOP-Lox-mGFP allele to label these neurons and their projections with mGFP (Hippenmeyer et al., 2005). At E14 and E16, we found the extent of radial migration into the developing cerebral wall was

identical in control and Arl13b-deficient neurons, which did possess cilia (Figure 1 E-F; Figure S1 K). At postnatal day 0 (P0), when projection neurons are terminating their migration, we saw no changes in neuronal placement or layer specification using layer-specific markers Cux 1 (layers 2–4), Ctip2 (layer 5), Brn1 (layers 2–4) and Tbr1 (layer 6) between control and Arl13b-deficient cortex (Figure 1 A-D). Once neurons reach their laminar destination, they establish functional connections by extending axons and dendrites and forming synapses. We observed generally normal patterns of extension and fasciculation of major subcerebral and cortico-cortical axonal pathways in Arl13b$^{Lox/Lox}$; Nex-Cre; mGFP mice at E16, P0, and P7 (Figure 1 G-R). However, we did notice a consistent decrease in the number of axonal bundles in the internal capsule at P0 and P7 (Figure 1 M-N, Q-R), as well as disruptions in callosal projections (data not shown). Together, these findings suggest that loss of Arl13b function does not affect the migration of cortical projection neurons, but results in subtle disruptions in post-migratory axonal outgrowth and connectivity of selective subsets of projection neurons.

Conditional deletion of Arll13b disrupts interneuronal placement but not post-migratory differentiation in the developing cerebral cortex

To determine the role of Arl13b in interneuron placement, we examined the cortex from Arl13b$^{Lox/Lox}$; Dlx5/6-Cre-IRES-EGFP (Dlx5/6-CIE) mice at postnatal day 10, when most cortical interneurons have terminated their migration and radial distribution within the cortical layers (Miyoshi and Fishell, 2011). By co-immunolabeling Creexpressing GFP^{+} interneurons with the interneuronal marker GABA in the somatosensory cortex, we saw a change in the positioning GABA/GFP double-positive cells, with a 39% decrease in the distribution of double-positive cells in layer VI with respect to the other layers in Arl13b$^{Lox/Lox}$; Dlx5/6-CIE mice (Figure 2A, B, G). Further, co-labeling with interneuron subtype markers calretinin and somatostatin indicated a 2.5-fold increase in the distribution of calretinin/GFP double-positive cells in layers II & III and a 4.2-fold increase in somatostatin/GFP double-positive cells in layer V of Arl13b$^{Lox/Lox}$; Dlx5/6-CIE somatosensory cortex (Figure 2C-F, H-I).

We also deleted Arl13b in the majority of post- migratory cortical interneurons (parvalbumin^{+}) starting around P8, using Parvalbumin-Cre line (Ascoli et al., 2008; Hippenmeyer et al., 2005) but observed no changes in either the numbers or distribution of interneuron subtypes or in the dendritic number, length or morphology of Arl13b-deficient interneurons compared to controls (Figure S2). Together, these observations indicate that normal Arl13b activity is specifically required for appropriate interneuronal placement within the cortex, but not for early post-migratory interneuronal differentiation.

Conditional deletion of Arll13b disrupts interneuronal migration in the developing cerebral cortex

We next examined Arl13b$^{Lox/Lox}$;Dlx5/6-CIE mice at times when interneurons are actively migrating into the cortex. At E14.5, mutant interneurons clustered at the pallial-subpallial boundary instead of exiting the ganglionic eminence (GE) and migrating into the dorsal cortex like control cells (Figure 3A, B and D). The number of GFP^{+} interneurons entering the dorsal cortex from the GE was significantly reduced in the Arl13b$^{Lox/Lox}$; Dlx5/6-CIE mutants (87 ± 3 cells/100 μm^3 for Arl13b$^{Lox/Lox}$ vs. 185 ± 12 cells/100 μm^3 for Arl13b$^{Lox/+}$). Normally, as interneurons migrate from the GE into the dorsal cortex, streams of migrating neurons can be seen in the marginal zone (MZ), intermediate zone (IZ), and subventricular zone (SVZ). We found fewer mutant interneurons in these migratory streams in mutants (compare Figure 3C with Figure 3D; Movies S1–2). We noticed a selective loss of interneurons migrating through the MZ region with a corresponding increase in the percentage of interneurons traversing the IZ (Figure 3E-G). The extent of interneuronal

migration from the pallial-subpallial boundary into the dorsal cerebral wall was significantly reduced in the mutants (Figure 3E-F; 929 μm ± 58 μm for Arl13b$^{Lox/Lox}$ vs. 1223 μm ± 47 μm for Arl13b$^{Lox/+}$). Moreover, mutant interneurons showed more processes extending from the cell soma as well as increased branching (Figure 3 H-L), but their overall branch length was decreased (Figure 3K). The same patterns of interneuron migration defects persist at E16 (Figure S3 A-D). The altered path, decreased distance traveled, and aberrant branching of mutant interneurons indicate that their migration is disrupted in the absence of Arl13b.

We confirmed this phenotype using a different Cre line, Nkx2.1-Cre, which is expressed beginning at E10.5 in both interneuronal progenitors and postmitotic interneurons of MGE and preoptic area (Xu et al., 2008). Similar to Arl13b$^{Lox/Lox}$;Dlx5/6-CIE brains, we observed defects in migration of both calbindin^{+} and Dlx2^{+} interneurons into the cortical wall at E14.5 and in the placement of GABA^{+} interneurons P10 cortex in the Arl13b$^{Lox/Lox}$; Nkx 2.1-Cre mutants(Figure S3 E-K). We saw no significant changes in cell proliferation or cortical cell death using antibodies against the mitotic marker PH3 or apoptotic marker cleaved caspase3^{+} (data not shown) indicating the reduction in cortical interneurons migrating in the cortex in either Arl13b$^{Lox/Lox}$;Dlx5/6-CIE mutants or Arl13b$^{Lox/Lox}$; Nkx 2.1-Cre was not a result of changes in either interneuronal generation or survival.

Altered dynamics of interneuronal migration following interneuron-specific inactivation of Arl13b

To gain insight into the dynamics of the migration defect in Arl13b$^{Lox/Lox}$;Dlx5/6-CIE interneurons in real time, we performed timelapse imaging of interneuronal migration in E14.5 mutant and control cortices. The streaming of interneurons from the GE into the cortex was altered in Arl13b$^{Lox/Lox}$;Dlx5/6-CIE brains (Movie S1). In medial regions of the cortex that contain the leading front of migrating cohorts of interneurons, we were able to clearly track the migratory behavior of individual GFP^{+} interneurons. In control slices, we observed robust migration in the MZ and IZ streams. Interneurons frequently exited the IZ stream, migrated radially and entered the MZ stream, where they resumed tangential migration. In the mutant cortices, however, the characteristic interneuron migratory streams were greatly reduced, with a less well-defined stream in the IZ and fewer motile neurons in the MZ (Movie S2).

Our analysis of individual neurons revealed that mutant interneurons underwent the typical mechanics of tangential migration: extension of the branched leading process, movement of the cytoplasmic swelling into the process, followed by somal translocation. However, mutant neurons underwent 49±0.5% fewer translocation events per hour than control cells. The periods of pausing were often characterized by the neurons sequentially extending leading processes in multiple directions without any accompanying somal translocation events. Therefore, we measured the rate of migration and found that Arl13b$^{Lox/Lox}$;Dlx5/6-CIE interneurons (24.6±1.2μm/h) migrated 29% slower than control cells (34.2±0.6μm/h).

When interneurons arrive near their final areal position in the dorsal cortex, they turn and radially migrate to their final position within the cortical plate (Nadarajah et al., 2003; Yokota et al., 2007). Live imaging at E16.5 showed clear cortical plate-directed movement of interneurons in the IZ of control slices, but interneurons in mutant slices moved more randomly (Movie S3). We measured the orientation of leading processes in control and mutant interneurons and found that 62 ± 0.6% of Arl13b$^{Lox/+}$;Dlx5/6-CIE interneurons in the IZ displayed a leading process that was oriented towards the cortical plate. In Arl13b$^{Lox/Lox}$;Dlx5/6-CIE interneurons, however, only 36 ± 2.7% were oriented towards the cortical plate. Together, these real time observations suggest that Arl13b is critical for the oriented navigation and migration of interneurons in the developing cerebral cortex.

Primary cilia function is required for interneuronal navigation through gradients of guidance cues

To determine whether the defective migration of Arl13b mutant interneurons is partly due to their inability to sense and respond to extrinsic migration guidance cues released by dorsal cortical cells (Valiente and Marin, 2010), we examined the ability of control and mutant interneurons to respond to gradients of such cues using a microfluidics chamber. This microscale device allowed us to present dorsal cortical cell-derived gradients of migration-regulating cues to isolated interneurons and to assay their response to these cues in a defined microenvironment (Taylor and Jeon, 2010). Here, interneurons and dorsal cortical cells are physically separated in two separate channels and interneurons are exposed to a microfluidic gradient of signals secreted by dorsal cortical cells in the opposing channel (Figure 4A). Under control conditions, interneurons migrate towards the dorsal cortical cells (Figure 4B). In contrast, the extent of migration of $Arl13b^{Lox/Lox}$; Dlx5/6-CIE interneurons towards dorsal cortical cells was significantly reduced (Figure 4C-D). Further, compared to control interneurons, migration of Arl13b null interneurons was also perturbed (Figure 4E-G). Together, these results suggest that the disruption of Arl13b in interneurons perturbs their ability to sense and respond to extrinsic guidance cues present in dorsal cortex that are necessary for the appropriate navigation into the cerebral wall.

Disruption of primary cilium localization of Arl13b disrupts interneuronal migration

To investigate whether the requirement for Arl13b in interneuron migration is specifically due to its ciliary role, we generated a non-ciliary form of Arl13b, $Arl13b^{V358A}$ (Figure 5A). The Arl13b V358A variant retains its GTPase activity but does not localize to cilia (Figure 5B), due to disruption of its VxPx motif (Deretic et al., 1998). $Arl13b^{V358A}$ could not rescue the migratory defects in Arl13b deficient interneurons (Figure 5C). Likewise, electroporating the Arl13b N-terminal domain (1-190aa; Arl13b-ND), which prevents Arl13b localization to cilia and maintenance of the primary cilium (Hori et al., 2008), into the GE of E14.5 embryos impaired the migration of the electroporated interneurons into the dorsal cortex (Figure 5D-F, H-I). Compared to the EGFP-electroporated control, 66% fewer Arl13b-ND expressing interneurons entered the dorsal cortex (15 ± 2.46 interneurons entered the dorsal cortex per slice electroporated with EGFP vs. 5 ± 0.80 electroporated with Arl13b-ND; n=35 slices). The migration index, calculated as the % change in interneurons that migrated greater than 350 μm past the GE-dorsal cortex boundary, was reduced by 72% in Arl13b-ND-$EGFP^{+}$ interneurons (Figure 5G). These results suggest that primary ciliary localization of Arl13b is required for efficient interneuronal migration into the dorsal cortex.

To confirm that the Arl13b effects on interneurons depend on primary cilia, we analysed the embryonic cortex of *Ift88* null mutants, which lack cilia and die by E11.5. (Pazour et al., 2000). Despite the likelihood of interneuron generation itself being affected in *Ift88* mutants, we found the migration of $Ift88^{-/-}$ interneurons into the cerebral wall was severely disrupted (Figure 5J-K). As conditional deletion of Ift88 in post-mitotic interneurons failed to ablate cilia (data not shown), we corroborated this using a small molecule inhibitor (HPI-4) that prevents ciliogenesis and truncates existing cilia (Hyman et al., 2009) (Figure S4). Together, these studies demonstrate that primary cilia activities involving Arl13b are critical for interneuron migration.

Interneuronal primary cilia show dynamic changes in length and orientation during migration

Primary cilia morphology, length and orientation, are linked to cilia-mediated signaling (Besschetnova et al., 2010; Ishikawa and Marshall, 2011) leading us to investigate the morphological dynamics of primary cilia in migrating interneurons in real time. We labeled interneuronal primary cilia with a Smoothened-tdTomato (Smo-Tom) fusion construct in the

MGE of Arl13b$^{Lox/+}$;Dlx5/6-CIE or Arl13b$^{Lox/Lox}$; Dlx5/6-CIE cortices and used timelapse imaging on a confocal microscope (Kim et al., 2010). Primary cilia in migrating interneurons are dynamic; they undergo repeated changes in length and position in stationary and moving neurons (Movies S4). We noticed that the cilia in control Arl13b$^{Lox/+}$;Dlx5/6-CIE interneurons were, on average, 35% longer than in mutant Arl13b$^{Lox/Lox}$;Dlx5/6-CIE interneurons (4.78 μm ± 0.75 μm, Arl13b$^{Lox/+}$; 3.08 μm ± 0.70 μm, Arl13b$^{Lox/Lox}$; n=35 control, 43 mutant cells). In addition, we found that dynamic changes in cilia morphology correlated with the migratory behavior of interneurons. For example, in both Arl13b$^{Lox/+}$; Dlx5/6-CIE and Arl13b$^{Lox/Lox}$; Dlx5/6-CIE interneurons, cilia predominantly localized to the soma of stationary cells and to the leading process of moving cells (during 66% ± 9.6% of the time spent moving, the primary cilia were found in or near the base of the leading process; during periods of pausing, the cilia were located in the cell soma 62% ± 6.6% of the time). Pausing interneurons displayed dynamic cilia that elongated, shortened, and rotated more than in moving interneurons (Movie S4). In pausing control interneurons, cilia were, on average, 23% longer than in moving cells (5.07 μm ± 0.87 μm in pausing neurons; 3.92 μm ± 1.51 μm in moving neurons, n=35 cells/group), and the dynamic range of cilia length was 59% greater (4.44 μm ± 0.73 μm) than in moving neurons (1.83 μm ± 0.58 μm). Consistent with these live imaging observations, we noticed primary cilia of differing lengths in fixed embryonic interneurons (Figure S5).

In contrast, primary cilia dynamics in Arl13b mutant interneurons were significantly altered (Movie S5). Cilia in pausing cells were only marginally (3.8%) longer than in moving cells (3.13 μm ± 0.76 μm, stationary; 3.01 μm ± 1.40 μm, moving; n=43 cells/group). In addition, the dynamic range of cilia length in pausing cells (2.02 ± 0.41 μm; n=16) was not significantly different from that of moving cells (2.46 μm ± 1.39 μm; n=27), but was significantly different from cilia in control neurons (4.44 μm ± 0.73 μm). These observations demonstrate that the primary cilia in migrating interneurons are morphologically dynamic, and that the dynamicity might correlate with the interneuron's phase of migration. Importantly, Arl13b mutant interneurons with defective migration display aberrant primary cilia dynamics during migration.

Localization of guidance cue receptors in the primary cilia of interneurons

We examined whether the receptors for guidance cues that are known to regulate interneuronal migration localize to the primary cilia of interneurons during migration. We labeled the primary cilia of Arl13b$^{Lox/+}$;Dlx5/6-CIE and Arl13b$^{Lox/Lox}$;Dlx5/6-CIE interneurons via electroporation with Smo-Tom. We then mapped the interneuronal cilia localization of the following receptors known to be critical for interneuron migration: BDNF receptor TrkB, GDNF receptor GFRα-1, SDF-1 receptors CXCR4 and CXCR7, NRG-1 receptor ErbB4, serotonin receptor 6 [5-Htr6], Slit receptors Robo1 and 2, and HGF/SF receptor MET (reviewed in Valiente and Marin, 2010; Sanchez-Alcaniz et al., 2011; Wang et al., 2011, Riccio et al., 2009) (Figure 6A-B). All of the guidance cue receptors that we tested localized to primary cilia in both mutant and control interneurons, but with different frequencies (Figure 6C). For each receptor, we observed differences in the percentage of primary cilia showing guidance cue receptor localization in mutant interneurons compared to control interneurons. We also examined the localization of the signaling receptors in ciliated mouse embryonic fibroblasts (MEFs) in which we could induce Arl13b deletion and found similar changes in the frequency of signaling receptor cilia localization. These changes in the distribution of signaling receptors upon Arl13b deletion support the hypothesis that the concentration of critical signaling receptors in primary cilia may promote their ability to function as sensors and conveyors of migration-regulating signals to interneurons during corticogenesis. Consistent with this hypothesis, we detected an increase in cAMP levels and decreased Erk phosphorylation in Arl13b mutant interneurons. These

two second messenger pathways are critical for interneuron migration and are downstream of many of the IN migration regulating receptors described above (Garzotto et al., 2008; Grabert and Wahle, 2008; Imamura et al., 2010; Lysko et al., 2011; Samuels et al., 2008; Sanchez-Alcaniz et al., 2011; Segarra et al., 2006; Wang et al., 2011).

Analysis of guidance cue receptor dynamics in Arl13b mutant cilia

In *C. elegans*, the orthologue of Arl13b, ARL-13 regulates intraflagellar transport (IFT) (Li et al., 2010) and is required for the stable localization of ciliary transmembrane proteins (Cevik et al., 2010). To investigate whether Arl13b modulates the transport and localization of transmembrane interneuronal guidance cue receptors into and within the cilium, we used fluorescence recovery after photobleaching (FRAP) to measure the movement of GFP-tagged serotonin receptor 6 (5-Htr6), which regulates interneuron migration (Riccio et al., 2009), within the primary cilia of control and Arl13b protein null (*Arl13b*^{hnn}) MEFs (Caspary et al., 2007). 5-Htr6-GFP localizes to the primary cilia in both wild-type and *Arl13b*^{hnn} cells (Figure 7A-B) and serves as a useful molecular tool to explore the receptor dynamics within primary cilia. Compared to wild-type cells, 27% fewer *Arl13b*^{hnn} MEFs localized 5-Htr6-GFP to the cilium. Photobleaching of a subregion of 5-Htr6-GFP-containing cilia revealed that cells lacking Arl13b show a 2-fold increase in recovery half-time (1.76 s ± 0.30 s in Arl13b WT vs. 3.63 s ± 0.44 s in *Arl13b*^{hnn}; n=14 [WT])(Figure 7C-D, Movie S6). The increase in recovery time was specific to receptor movement within mutant primary cilia; FRAP rates of 5-Htr6-GFP localized to nonciliary membranes of Arl13b null cells were similar to wild-type rates (WT, 1.04 s ± 0.15 s; Arl13b$^{-/-}$, 1.19 s ± 0.09 s). These data suggest that Arl13b is required for the efficient ciliary movement and localization of interneuronal migration guidance cue receptors such as 5-Htr6.

Expression of mutated human Arl13b disrupts interneuron migration

Three distinct mutations in Arl13b have been identified in Joubert syndrome patients (Cantagrel et al., 2008). The R79Q substitution interferes with GTP binding, W82X introduces a stop codon in exon 3 and R200C generates a missense mutation within the C-terminal coiled-coiled domain of Arl13b (Figure 8A). To test whether expression of the mutated forms of human Arl13b could affect interneuron migration, we focally electroporated wild-type human or mutant human ARL13b constructs tagged with tdTomato into the GE of Dlx-Cre, Arl13b$^{Lox/Lox}$ E14.5 cortex. While wild type human ARL13B rescued the migratory defects in the mutant cells, none of the ARL13B patient variants did (Figure 8), suggesting that the human mutations in Arl13b may affect IN migration in Joubert syndrome patients. Anti-caspase labeling indicates that cells expressing human mutant Arl13b are not apoptotic (data not shown). Together, these studies demonstrate that expression of disease alleles of human Arl13b in interneurons can disrupt their migration.

DISCUSSION

Disrupted primary cilia function in humans results in profound cortical abnormalities and cognitive deficits (Hildebrandt et al., 2011; Louvi and Grove, 2011). Nevertheless, the role of cilia function in cortical neuronal organization remains unknown. Here we show that primary cilia play a guiding role in the development and placement of interneurons during the construction of cerebral cortex.

By using Arl13b, we gained a entry point for understanding the role of cilia in cortical development since Arl13b mutants impair but do not destroy the cilia and downstream pathways. Our results provide new insights into the etiology of the neurodevelopmental defects found in ciliopathies. It is well established that altered integration of interneurons into the cortical network and the resultant changes in brain's excitatory/inhibitory balance

can lead to developmental neuropsychiatric disorders like autism spectrum disorders, epilepsy and schizophrenia (Batista-Brito and Fishell, 2009; Manzini and Walsh, 2011; Metin et al., 2008; Valiente and Marin, 2010; Wynshaw-Boris et al., 2010; Yizhar et al., 2011). Importantly, these disorders have been associated with Joubert syndrome (Lee and Gleeson, 2011; Sattar and Gleeson, 2011). Our data suggest that defective interneuron migration and placement following Arl13b deletion may disrupt the appropriate elaboration of cortical inhibitory network, thus contributing to altered cortical inhibition and neurobehavioral deficits in Arl13b-related ciliopathies. Furthermore, appropriate radial distribution and integration of diverse subtypes of GABAergic interneurons into distinct laminar locations occurs during early post-natal development (De Marco Garcia et al., 2011; Lodato et al., 2011; Miyoshi and Fishell, 2011). The altered distribution of GABA, calretinin and somatostatin expressing interneurons in Arl13b mutants is suggestive of a potential role for Arl13b in interneuron subtype migration or the emergence of migration-related interneuron subtype identity.

The distinct roles of Arl13b activity for interneuron and projection neuron migration may reflect the fundamental differences in the way these two major classes of cortical neurons migrate. Projection neurons migrate primarily using radial glial guides as substrates, whereas interneurons rely extensively on extracellular, non-substrate-based guidance cues for their migration into the cerebral wall (Valiente and Marin, 2010). Primary cilia activity might be more critical for cell migration that depends on sensing extracellular guidance cues and less so for substrate contact-guided migration.

Our results emphasize a role for cilia in early cortical development. However, the disruption in the major subcerebral axonal projections (i.e., internal capsule) of pyramidal neurons in Arl13b mutants may be related to a role for Arl13b^{+} cilia in the post-migratory identity and differentiation of subsets of projection neurons. Alternatively, it may also be the result of a yet to be uncovered, non-cilia role for Arl13bin axon growth in a subset of projection neurons. Disrupted cortico-spinal axonal axonal connectivity is also seen in Joubert syndrome patients (Engle, 2010; Poretti et al., 2007) and primary cilia-specific activities of Arl13b in pyramidal neurons may underlie some aspects of this defect.

One surprising finding is how dynamic the primary cilia are, not only do they change in length, they also rotate, branch, and appear to probe their surroundings. This is quite distinct from true motile cilia; ependymal cilia beat rhythmically to form a guidance molecule concentration gradient in the CSF that directs the migration of adult neuroblasts (Sawamoto et al., 2006). Interneuronal primary cilia likely bind and transduce signals from gradients of guidance molecules in a cell autonomous fashion that leads to changes in interneuronal morphology and movement. In fact, we found that cilia in wild-type interneurons localized to the leading process during migration, but moved closer to the cell body during periods of pausing when they became much more dynamic in their movement and length. In contrast, primary cilia in Arl13b-deficient interneurons did not display such dynamism. Considering that mutant interneurons paused longer during migration, extended increased number of processes in multiple directions, and were unable to respond to microgradients of guidance cues, the reduction in cilia dynamics may reflect an inability to efficiently sense guidance cues in the migratory environment. This is further supported by the disrupted localization of multiple signaling receptors in Arl13b-deficient interneuronal cilia.

The mechanism(s) underlying the misdistribution of guidance cue receptors in Arl13b-deficient cilia remains unclear. Another protein implicated in Joubert syndrome, the transition zone protein, Tctn1, regulates Arl13b localization to the cilium in neurons (Garcia-Gonzalo et al., 2011). Moreover, *C. elegans* ARL-13 regulates IFT by maintaining the association between IFT subcomplexes A and B and associates with the ciliary

membrane via its palmitoylation motifs (Li et al., 2010; Cevik et al., 2010). Together, these data suggest that Arl13b's links to the IFT complexes, ciliary transmembrane receptor localization, and the ciliary transition zone may help promote the retention and distribution of crucial receptor molecules within the primary cilium of interneurons. Detailed understanding of such a model and its relevance for the regulation of diverse patterns of interneuron subtype migration will await more refined genetic and molecular tools that would allow cilia specific signaling manipulation in specific subsets of interneurons in the early embryonic brain. But consistent with this idea, we detected an increase in cAMP levels along with a decrease in Erk phosphorylation when we examined the total population of Arl13b mutant interneurons. Both of these pathways are downstream of several interneuron migration regulating receptors (Garzotto et al., 2008; Grabert and Wahle, 2008; Imamura et al., 2010; Lysko et al., 2011; Samuels et al., 2008; Sanchez-Alcaniz et al., 2011; Segarra et al., 2006; Stanco et al., 2009; Wang et al., 2011). Increased cAMP levels can disrupt the branching of migrating interneurons, and decreased ERK phosphorylation is associated with retarded interneuron migration (Lysko et al., 2011; Imamura et al., 2010). Although the current evidence on Arl13b suggests that ciliary localization of multiple signaling receptors are perturbed in Arl13 mutants, future identification of IN migration related ligand-receptor combination or receptor subtypes (e.g., GPCRs) that are preferentially affected in Arl13b mutants will help further define the specific signaling pathways that may be defective in Arl13b deficient primary cilia.

This hypothesis raises important questions about how directional information from guidance cues is conveyed through the cilium to lead to changes in interneuron migration. Also, what advantages does the cell gain by relying on such a small organelle to transduce extracellular signals? The primary cilium is structured and positioned to be able to generate a fast and robust response to extracellular signals. The diffusion barrier at the base of the cilium allows a cell to maximize the local concentration of guidance cue receptors and their downstream effectors within cilia. Thus, high levels of second messengers could be sustained more easily within the narrow geometry of the cilium than in other regions of the cell where diffusion through a larger space could lead to a rapid diminishment of the signal. In addition, the cilium's proximity to the nucleus and its link to the centrosome-associated microtubule network could promote rapid and efficient signal transduction during nucleokinesis associated with interneuron migration. Consistently, pericentrin, a member of the centrosomal complex necessary for neuronal cilia formation (Miyoshi et al., 2009), is crucial for tangential neuronal migration (Endoh-Yamagami et al., 2010). However, it remains untested if primary cilia and the growth cones in the leading processes of migrating interneurons transduce different signals related to directed cell movement. They may differentially affect the chemotaxic and haptotaxic components of interneuron migration. Understanding the cross-talk that occurs between intracellular signaling cascades that originate in each of these cellular compartments during interneuron movement will help delineate the primary cilia-specific pathways mediating interneuron development. Furthermore, it will be crucial to examine the differences in the activities of receptors that are localized exclusively in one or in both primary cilia and growth cones during interneuron migration. Nevertheless, the evidence we present in this study demonstrates a role for primary cilia in neuronal development and cerebral cortical organization. Moreover, it provides a neurodevelopmental basis for the functional deficits observed in Joubert syndrome patients.

Materials and Methods

MICE

Mice were cared for under protocols approved by the University of North Carolina and Emory University. Lines used were: Arl13b^{tm1Tc}, MGI: 4948239 (Su et al., 2012), Nex-Cre

(Goebbels et al., 2006), Dlx5/6-CIE (Stenman et al., 2003), Parv-Cre (Hippenmeyer et al., 2005), Tau-Lox-STOP-Lox-GFP (Hippenmeyer et al., 2005), Nkx2.1-Cre (Xu et al., 2008), Ift88$^{Lox/Lox}$ (Haycraft et al., 2007), and CAGG-CreER™ (JAX: 004682; Hayashi and McMahon, 2002).

IMMUNOHISTOCHEMISTRY

Cerebral cortical sections and cortical cells were immunolabeled as previously described (Schmid et al., 2003; Yokota et al., 2007, 2009). List of primary antibodies used are provided in the supplemental information. Secondary antibodies were AlexaFluor 488 or Cy3-conjugated (Invitrogen and Jackson ImmunoResearch). Nuclei were counterstained with DRAQ5 (Biostatus Limited).

Live-imaging of interneuronal migration and primary cilia activity in interneurons—GFP^{+} interneurons, Smo-tdTomato^{+} interneuronal primary cilia, or interneurons expressing ARL13B patient variants in embryonic cortices were live imaged using a Zeiss LSM710 inverted confocal laser-scanning microscope or an Olympus Fluo-View FV1000 inverted confocal laser-scanning system attached to a live-cell incubation chamber.

Microfluidic chamber assay for interneuronal migration—Interneurons seeded onto microfluidic chambers (Taylor and Jeon, 2010) were used probe the ability these neurons to respond to extrinsic migration guidance cue gradients released by dorsal cortical cells. Details of this microfluidics assay are provided in the supplemental information.

Inducible deletion of Arl13b in mouse embryonic fibroblasts (MEFs)—MEFs were isolated from E12.5 control Arl13b$^{Lox/Lox}$ or Arl13b$^{Lox/Lox}$; CAGG-CreER™ embryos as previously described. MEFs were serum-starved for 24 hours and tamoxifen (2μM, Sigma H7904) was added in serum-free media. Cover slips were collected 48 hours after tamoxifen treatment and MEFs were fixed and processed for antibody staining.

Fluorescent recovery after photobleaching (FRAP) analysis—Wild-type and *Arl13b*$^{hnn/hnn}$ MEFs were grown in DMEM/10% FBS and co-transfected with pCAGS-dsRed and pCAGS-Htr6-GFP (a gift from Dr. Kirk Mykytyn, Ohio State University). FRAP was carried out after 48 hours of serum starvation using the Olympus FluoView 1000 live cell confocal system. After the acquisition of basal state images, the region of interest (ROI) was photobleached with a 800 m.sec pulse of 488nm laser, followed by rapid, repetitive acquisition of the recovery of GFP fluorescence in the ROI. Data was analyzed using the Igor Pro 6.12A (Wavemetrics, Inc.) software to determine the recovery half-time and evaluate the dynamics of receptor movement within primary cilium.

Measurement of cAMP levels—cAMP levels in the ganglionic eminence extracts from Arl13b$^{Lox/+}$;Dlx5/6-CIE or Arl13b$^{Lox/Lox}$;Dlx5/6-CIE brains (E16) were measured as described in the manufacturer's instructions (R&D Systems). Extracts contained equal levels of GFP.

Supplementary Material

Refer to Web version on PubMed Central for supplementary material.

Acknowledgments

This research was supported by NIH grants MH060929 to EA and NS056380 to TC, a NARSAD Young Investigator Award to HH and by the confocal imaging core of an NINDS institutional center core grant. We are

especially grateful to Drs. Bradley Yoder, Hisham Bazzi and Kathryn Anderson for providing the Ift88 deficient embryos. We thank A- S. Lamantia, L. Pevny, M. Deshmukh, and W. Snider for helpful comments and C. Strauss for editing.

References

Amador-Arjona A, Elliott J, Miller A, Ginbey A, Pazour GJ, Enikolopov G, Roberts AJ, Terskikh AV. Primary cilia regulate proliferation of amplifying progenitors in adult hippocampus: implications for learning and memory. J Neurosci. 2011; 31:9933–9944. [PubMed: 21734285]

Arellano JI, Guadiana SM, Breunig JJ, Rakic P, Sarkisian MR. Development and distribution of neuronal cilia in mouse neocortex. J Comp Neurol. 2012

Ascoli GA, Alonso-Nanclares L, Anderson SA, Barrionuevo G, Benavides-Piccione R, Burkhalter A, Buzsaki G, Cauli B, Defelipe J, Fairen A, et al. Petilla terminology: nomenclature of features of GABAergic interneurons of the cerebral cortex. Nat Rev Neurosci. 2008; 9:557–568. [PubMed: 18568015]

Ayala R, Shu T, Tsai LH. Trekking across the brain: the journey of neuronal migration. Cell. 2007; 128:29–43. [PubMed: 17218253]

Batista-Brito R, Fishell G. The developmental integration of cortical interneurons into a functional network. Curr Top Dev Biol. 2009; 87:81–118. [PubMed: 19427517]

Berbari NF, O'Connor AK, Haycraft CJ, Yoder BK. The primary cilium as a complex signaling center. Curr Biol. 2009; 19:R526–R535. [PubMed: 19602418]

Besschetnova TY, Kolpakova-Hart E, Guan Y, Zhou J, Olsen BR, Shah JV. Identification of signaling pathways regulating primary cilium length and flowmediated adaptation. Curr Biol. 2010; 20:182–187. [PubMed: 20096584]

Besse L, Neti M, Anselme I, Gerhardt C, Ruther U, Laclef C, Schneider-Maunoury S. Primary cilia control telencephalic patterning and morphogenesis via Gli3 proteolytic processing. Development. 2011; 138:2079–2088. [PubMed: 21490064]

Bishop GA, Berbari NF, Lewis J, Mykytyn K. Type III adenylyl cyclase localizes to primary cilia throughout the adult mouse brain. J Comp Neurol. 2007; 505:562–571. [PubMed: 17924533]

Breunig JJ, Sarkisian MR, Arellano JI, Morozov YM, Ayoub AE, Sojitra S, Wang B, Flavell RA, Rakic P, Town T. Primary cilia regulate hippocampal neurogenesis by mediating sonic hedgehog signaling. Proc Natl Acad Sci U S A. 2008; 105:13127–13132. [PubMed: 18728187]

Cantagrel V, Silhavy JL, Bielas SL, Swistun D, Marsh SE, Bertrand JY, Audollent S, Attie-Bitach T, Holden KR, Dobyns WB, et al. Mutations in the cilia gene ARL13B lead to the classical form of Joubert syndrome. Am J Hum Genet. 2008; 83:170–179. [PubMed: 18674751]

Caspary T, Larkins CE, Anderson KV. The graded response to Sonic Hedgehog depends on cilia architecture. Dev Cell. 2007; 12:767–778. [PubMed: 17488627]

Cevik S, Hori Y, Kaplan OI, Kida K, Toivenon T, Foley-Fisher C, Cottell D, Katada T, Kontani K, Blacque OE. Joubert syndrome Arl13b functions at ciliary membranes and stabilizes protein transport in Caenorhabditis elegans. J Cell Biol. 2010; 188:953–969. [PubMed: 20231383]

De Marco Garcia NV, Karayannis T, Fishell G. Neuronal activity is required for the development of specific cortical interneuron subtypes. Nature. 2011; 472:351–355. [PubMed: 21460837]

Deretic D, Schmerl S, Hargrave PA, Arendt A, McDowell JH. Regulation of sorting and post-Golgi trafficking of rhodopsin by its C-terminal sequence QVS(A)PA. Proc Natl Acad Sci U S A. 1998; 95:10620–10625. [PubMed: 9724753]

Endoh-Yamagami S, Karkar KM, May SR, Cobos I, Thwin MT, Long JE, Ashique AM, Zarbalis K, Rubenstein JL, Peterson AS. A mutation in the pericentrin gene causes abnormal interneuron migration to the olfactory bulb in mice. Dev Biol. 2010; 340:41–53. [PubMed: 20096683]

Engle EC. Human genetic disorders of axon guidance. Cold Spring Harb Perspect Biol. 2010; 2:a001784. [PubMed: 20300212]

Garcia-Gonzalo FR, Corbit KC, Sirerol-Piquer MS, Ramaswami G, Otto EA, Noriega TR, Seol AD, Robinson JF, Bennett CL, Josifova DJ, et al. A transition zone complex regulates mammalian ciliogenesis and ciliary membrane composition. Nat Genet. 2011; 43:776–784. [PubMed: 21725307]

Garzotto D, Giacobini P, Crepaldi T, Fasolo A, De Marchis S. Hepatocyte growth factor regulates migration of olfactory interneuron precursors in the rostral migratory stream through Met-Grb2 coupling. J Neurosci. 2008; 28:5901–5909. [PubMed: 18524894]

Goebbels S, Bormuth I, Bode U, Hermanson O, Schwab MH, Nave KA. Genetic targeting of principal neurons in neocortex and hippocampus of NEXCre mice. Genesis. 2006; 44:611–621. [PubMed: 17146780]

Grabert J, Wahle P. Neuronal activity and TrkB ligands influence Kv3.1b and Kv3.2 expression in developing cortical interneurons. Neuroscience. 2008; 156:618–629. [PubMed: 18775767]

Han YG, Alvarez-Buylla A. Role of primary cilia in brain development and cancer. Curr Opin Neurobiol. 2010; 20:58–67. [PubMed: 20080044]

Handel M, Schulz S, Stanarius A, Schreff M, Erdtmann-Vourliotis M, Schmidt H, Wolf G, Hollt V. Selective targeting of somatostatin receptor 3 to neuronal cilia. Neuroscience. 1999; 89:909–926. [PubMed: 10199624]

Haycraft CJ, Zhang Q, Song B, Jackson WS, Detloff PJ, Serra R, Yoder BK. Intraflagellar transport is essential for endochondral bone formation. Development. 2007; 134:307–16. [PubMed: 17166921]

Hayashi S, McMahon AP. Efficient recombination in diverse tissues by a tamoxifen-inducible form of Cre: a tool for temporally regulated gene activation/inactivation in the mouse. Dev Biol. 2002; 244:305–18. [PubMed: 11944939]

Higginbotham HR, Gleeson JG. The centrosome in neuronal development. Trends Neurosci. 2007; 30:276–283. [PubMed: 17420058]

Hildebrandt F, Benzing T, Katsanis N. Ciliopathies. N Engl J Med. 2011; 364:1533–1543. [PubMed: 21506742]

Hippenmeyer S, Vrieseling E, Sigrist M, Portmann T, Laengle C, Ladle DR, Arber S. A developmental switch in the response of DRG neurons to ETS transcription factor signaling. PLoS Biol. 2005; 3:e159. [PubMed: 15836427]

Hori Y, Kobayashi T, Kikko Y, Kontani K, Katada T. Domain architecture of the atypical Arf-family GTPase Arl13b involved in cilia formation. Biochem Biophys Res Commun. 2008; 373:119–124. [PubMed: 18554500]

Hyman JM, Firestone AJ, Heine VM, Zhao Y, Ocasio CA, Han K, Sun M, Rack PG, Sinha S, Wu JJ, et al. Small-molecule inhibitors reveal multiple strategies for Hedgehog pathway blockade. Proc Natl Acad Sci U S A. 2009; 106:14132–14137. [PubMed: 19666565]

Imamura O, Pages G, Pouyssegur J, Endo S, Takishima K. ERK1 and ERK2 are required for radial glial maintenance and cortical lamination. Genes Cells. 2010; 15:1072–1088. [PubMed: 20825492]

Ishikawa H, Marshall WF. Ciliogenesis: building the cell's antenna. Nat Rev Mol Cell Biol. 2011; 12:222–234. [PubMed: 21427764]

Kim J, Lee JE, Heynen-Genel S, Suyama E, Ono K, Lee K, Ideker T, Aza-Blanc P, Gleeson JG. Functional genomic screen for modulators of ciliogenesis and cilium length. Nature. 2010; 464:1048–1051. [PubMed: 20393563]

Lee JE, Gleeson JG. Cilia in the nervous system: linking cilia function and neurodevelopmental disorders. Curr Opin Neurol. 2011; 24:98–105. [PubMed: 21386674]

Li Y, Wei Q, Zhang Y, Ling K, Hu J. The small GTPases ARL-13 and ARL-3 coordinate intraflagellar transport and ciliogenesis. J Cell Biol. 2010; 189:1039–1051. [PubMed: 20530210]

Lodato S, Rouaux C, Quast KB, Jantrachotechatchawan C, Studer M, Hensch TK, Arlotta P. Excitatory projection neuron subtypes control the distribution of local inhibitory interneurons in the cerebral cortex. Neuron. 2011; 69:763–779. [PubMed: 21338885]

Louvi A, Grove EA. Cilia in the CNS: The Quiet Organelle Claims Center Stage. Neuron. 2011; 69:1046–1060. [PubMed: 21435552]

Lysko DE, Putt M, Golden JA. SDF1 regulates leading process branching and speed of migrating interneurons. J Neurosci. 2011; 31:1739–1745. [PubMed: 21289183]

Manzini MC, Walsh CA. What disorders of cortical development tell us about the cortex: one plus one does not always make two. Curr Opin Genet Dev. 2011; 21:333–339. [PubMed: 21288712]

Marin O, Valiente M, Ge X, Tsai LH. Guiding neuronal cell migrations. Cold Spring Harb Perspect Biol. 2010; 2:a001834. [PubMed: 20182622]

Metin C, Vallee RB, Rakic P, Bhide PG. Modes and mishaps of neuronal migration in the mammalian brain. J Neurosci. 2008; 28:11746–11752. [PubMed: 19005035]

Miyoshi G, Fishell G. GABAergic interneuron lineages selectively sort into specific cortical layers during early postnatal development. Cereb Cortex. 2011; 21:845–852. [PubMed: 20732898]

Miyoshi K, Kasahara K, Miyazaki I, Shimizu S, Taniguchi M, Matsuzaki S, Tohyama M, Asanuma M. Pericentrin, a centrosomal protein related to microcephalic primordial dwarfism, is required for olfactory cilia assembly in mice. FASEB J. 2009; 23:3289–3297. [PubMed: 19470799]

Nadarajah B, Alifragis P, Wong RO, Parnavelas JG. Neuronal migration in the developing cerebral cortex: observations based on real-time imaging. Cereb Cortex. 2003; 13:607–611. [PubMed: 12764035]

Pazour GJ, Dickert BL, Vucica Y, Seeley ES, Rosenbaum JL, Witman GB, Cole DG. Chlamydomonas IFT88 and its mouse homologue, polycystic kidney disease gene tg737, are required for assembly of cilia and flagella. J Cell Biol. 2000; 151:709–718. [PubMed: 11062270]

Pedersen LB, Rosenbaum JL. Intraflagellar transport (IFT) role in ciliary assembly, resorption and signalling. Curr Top Dev Biol. 2008; 85:23–61. [PubMed: 19147001]

Poretti A, Boltshauser E, Loenneker T, Valente EM, Brancati F, Il'yasov K, Huisman TA. Diffusion tensor imaging in Joubert syndrome. Am J Neuroradiol. 2007; 28:1929–1933. [PubMed: 17898198]

Rakic P. Mode of cell migration to the superficial layers of fetal monkey neocortex. J Comp Neurol. 1972; 145:61–83. [PubMed: 4624784]

Riccio O, Potter G, Walzer C, Vallet P, Szabo G, Vutskits L, Kiss JZ, Dayer AG. Excess of serotonin affects embryonic interneuron migration through activation of the serotonin receptor 6. Mol Psychiatry. 2009; 14:280–290. [PubMed: 18663366]

Rudy B, Fishell G, Lee S, Hjerling-Leffler J. Three groups of interneurons account for nearly 100% of neocortical GABAergic neurons. Dev Neurobiol. 2011; 71:45–61. [PubMed: 21154909]

Samuels IS, Karlo JC, Faruzzi AN, Pickering K, Herrup K, Sweatt JD, Saitta SC, Landreth GE. Deletion of ERK2 mitogen-activated protein kinase identifies its key roles in cortical neurogenesis and cognitive function. J Neurosci. 2008; 28:6983–6995. [PubMed: 18596172]

Sanchez-Alcaniz JA, Haege S, Mueller W, Pla R, Mackay F, Schulz S, Lopez-Bendito G, Stumm R, Marin O. Cxcr7 controls neuronal migration by regulating chemokine responsiveness. Neuron. 2011; 69:77–90. [PubMed: 21220100]

Sattar S, Gleeson JG. The ciliopathies in neuronal development: a clinical approach to investigation of Joubert syndrome and Joubert syndrome-related disorders. Dev Med Child Neurol. 2011; 53:793–798. [PubMed: 21679365]

Sawamoto K, Wichterle H, Gonzalez-Perez O, Cholfin JA, Yamada M, Spassky N, Murcia NS, Garcia-Verdugo JM, Marin O, Rubenstein JL, et al. New neurons follow the flow of cerebrospinal fluid in the adult brain. Science. 2006; 311:629–632. [PubMed: 16410488]

Schmid RS, McGrath B, Berechid BE, Boyles B, Marchionni M, Sestan N, Anton ES. Neuregulin 1-erbB2 signaling is required for the establishment of radial glia and their transformation into astrocytes in cerebral cortex. Proc Natl Acad Sci U S A. 2003; 100:4251–4256. [PubMed: 12649319]

Segarra J, Balenci L, Drenth T, Maina F, Lamballe F. Combined signaling through ERK, PI3K/AKT, and RAC1/p38 is required for met-triggered cortical neuron migration. J Biol Chem. 2006; 281:4771–4778. [PubMed: 16361255]

Solecki DJ, Model L, Gaetz J, Kapoor TM, Hatten ME. Par6alpha signaling controls glial-guided neuronal migration. Nat Neurosci. 2004; 7:1195–1203. [PubMed: 15475953]

Stanco A, Szekeres C, Patel N, Rao S, Campbell K, Kreidberg JA, Polleux F, Anton ES. Netrin-1-alpha3beta1 integrin interactions regulate the migration of interneurons through the cortical marginal zone. Proc. Natl. Acad. Sci. U.S.A. 2009; 106:7595–7600. [PubMed: 19383784]

Stenman J, Toresson H, Campbell K. Identification of two distinct progenitor populations in the lateral ganglionic eminence: implications for striatal and olfactory bulb neurogenesis. J Neurosci. 2003; 23:167–174. [PubMed: 12514213]

Su C, Bay SN, Mariani LE, Horner MJ, Caspary T. Temporal deletion of Arl13b reveals mispatterned neural tube corrects cell fate over time. Development. 2012 In press.

Taylor AM, Jeon NL. Micro-scale and microfluidic devices for neurobiology. Curr Opin Neurobiol. 2010; 20:640–647. [PubMed: 20739175]

Valiente M, Marin O. Neuronal migration mechanisms in development and disease. Curr Opin Neurobiol. 2010; 20:68–78. [PubMed: 20053546]

Wang Y, Li G, Stanco A, Long JE, Crawford D, Potter GB, Pleasure SJ, Behrens T, Rubenstein JL. CXCR4 and CXCR7 have distinct functions in regulating interneuron migration. Neuron. 2011; 69:61–76. [PubMed: 21220099]

Willaredt MA, Hasenpusch-Theil K, Gardner HA, Kitanovic I, Hirschfeld-Warneken VC, Gojak CP, Gorgas K, Bradford CL, Spatz J, Wolfl S, et al. A crucial role for primary cilia in cortical morphogenesis. J Neurosci. 2008; 28:12887–12900. [PubMed: 19036983]

Wilson SL, Wilson JP, Wang C, Wang B, McConnell SK. Primary cilia and Gli3 activity regulate cerebral cortical size. Dev Neurobiol. 2012; 72:1196–1212. [PubMed: 21976438]

Wu SX, Goebbels S, Nakamura K, Kometani K, Minato N, Kaneko T, Nave KA, Tamamaki N. Pyramidal neurons of upper cortical layers generated by NEX-positive progenitor cells in the subventricular zone. Proc Natl Acad Sci U S A. 2005; 102:17172–17177. [PubMed: 16284248]

Wynshaw-Boris A, Pramparo T, Youn YH, Hirotsune S. Lissencephaly: mechanistic insights from animal models and potential therapeutic strategies. Semin Cell Dev Biol. 2010; 21:823–830. [PubMed: 20688183]

Xu Q, Tam M, Anderson SA. Fate mapping Nkx2.1-lineage cells in the mouse telencephalon. J Comp Neurol. 2008; 506:16–29. [PubMed: 17990269]

Yizhar O, Fenno LE, Prigge M, Schneider F, Davidson TJ, O'Shea DJ, Sohal VS, Goshen I, Finkelstein J, Paz JT, et al. Neocortical excitation/inhibition balance in information processing and social dysfunction. Nature. 2011; 477:171–178. [PubMed: 21796121]

Yokota Y, Gashghaei HT, Han C, Watson H, Campbell KJ, Anton ES. Radial glial dependent and independent dynamics of interneuronal migration in the developing cerebral cortex. PLoS ONE. 2007; 2:e794. [PubMed: 17726524]

Yokota Y, Kim WY, Chen Y, Wang X, Stanco A, Komuro Y, Snider W, Anton ES. The adenomatous polyposis coli protein is an essential regulator of radial glial polarity and construction of the cerebral cortex. Neuron. 2009; 61:42–56. [PubMed: 19146812]

Highlights

- Arl13b cilia activity is required for interneuronal migration and placement
- Ciliary dynamics increase during decision- making pauses in migration
- Arl13b regulates guidance receptor localization and movement selectively in cilia
- Joubert Syndrome-causing Arl13b mutations affect interneuronal development

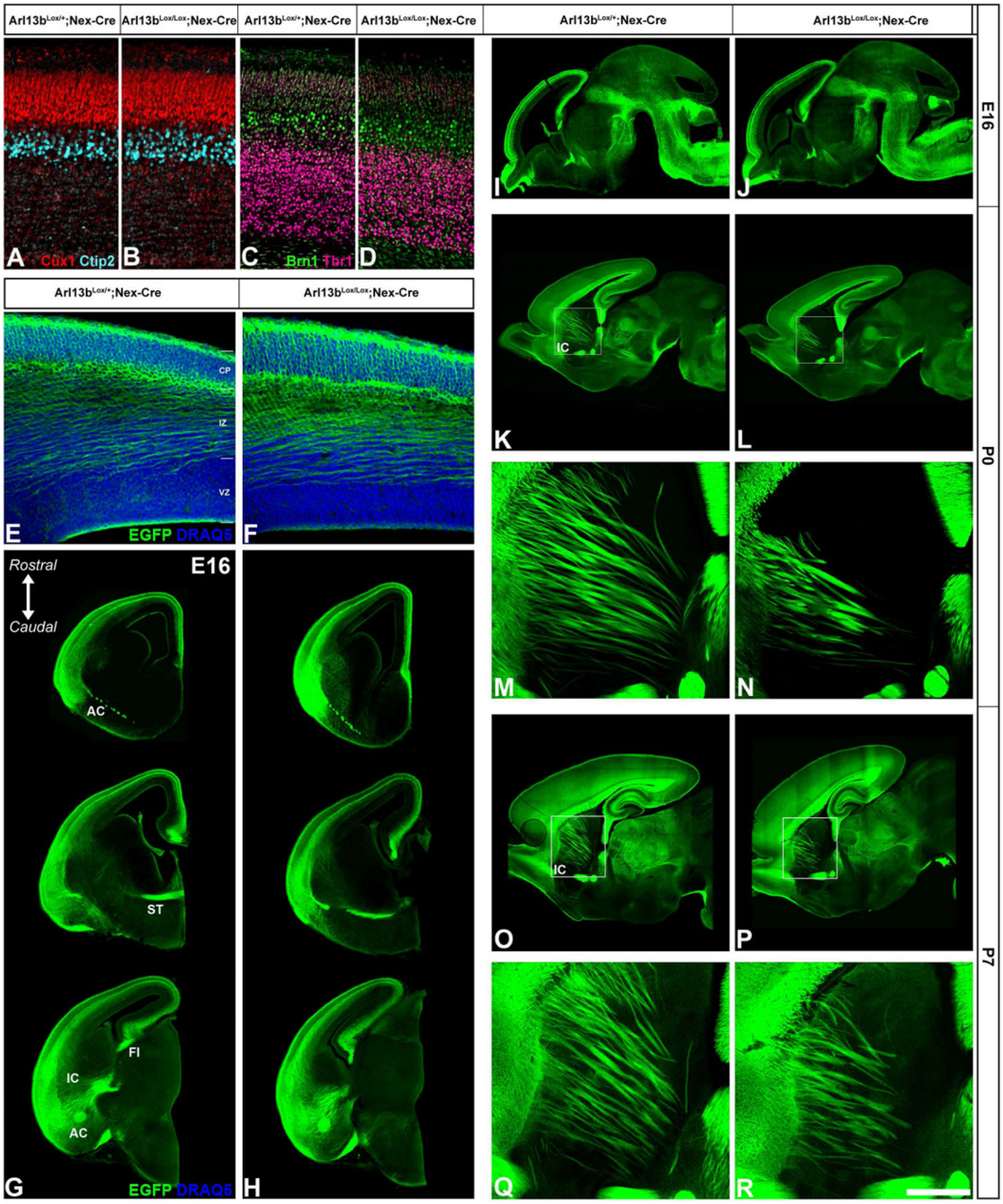

Figure 1. Projection neuron placement and axonal outgrowth in Nex-Cre; Arl13b$^{Lox/Lox}$ cortex

(A-D) P0 somatosensory cortex of Arl13b$^{Lox/+}$; Nex-Cre (A,C) or Arl13b$^{Lox/Lox}$; Nex-Cre (B,D) mice were immunolabeled for Cux1 (layers II-IV), Ctip2 (layer V), Brn1 (layers II-V) and Tbr1 (layer VI). Neuronal positioning was not altered by Arl13b deletion in projection neurons. (E, F) Serial coronal sections spanning the rostro-caudal extent of E16 Arl13b$^{Lox/+}$; Nex-Cre; Tau-mGFP (E) or Arl13b$^{Lox/Lox}$; Nex-Cre; Tau-mGFP (F) cortex were immunolabeled for mGFP. No differences in the extent of migration of GFP^{+} projection neurons were seen. Major cortical axonal tracts also appear normal in mutants. (G, H) High magnification image of sections from the lateral cortex of E16 Arl13b$^{Lox/+}$; Nex-Cre; Tau-mGFP (G) or Arl13b$^{Lox/Lox}$; Nex-Cre; Tau-mGFP (H) cortex immunolabeled for mGFP

showing normal migration and initial axonal growth of projection neurons. (I-R) Sagittal sections from E16 (I, J), P0 (K-N) and P7 (O-R) Arl13b$^{Lox/+}$; Nex-Cre; Tau-mGFP (I, K, M, O, Q) or Arl13b$^{Lox/Lox}$;Nex-Cre; Tau-mGFP (J, L, N, P, R) cortex indicates generally normal development of major cortical axonal tracts. (M-N, Q-R) However, high magnification of internal capsule regions outlined in K-L and O-P, respectively, illustrates disrupted fasciculation in mutants. Sections in G and H were counterstained with DRAQ5 (nuclei). VZ-ventricular zone, IZ-intermediate zone, CP-cortical plate, CC-corpus callosum, IC-internal capsule, FI-fimbria, ST-stria terminalis, AC-anterior commissure. Scale bar=A-D, 225 μm; E-F, M-N, Q-R, 300μm; GL, O-P, 750μm.

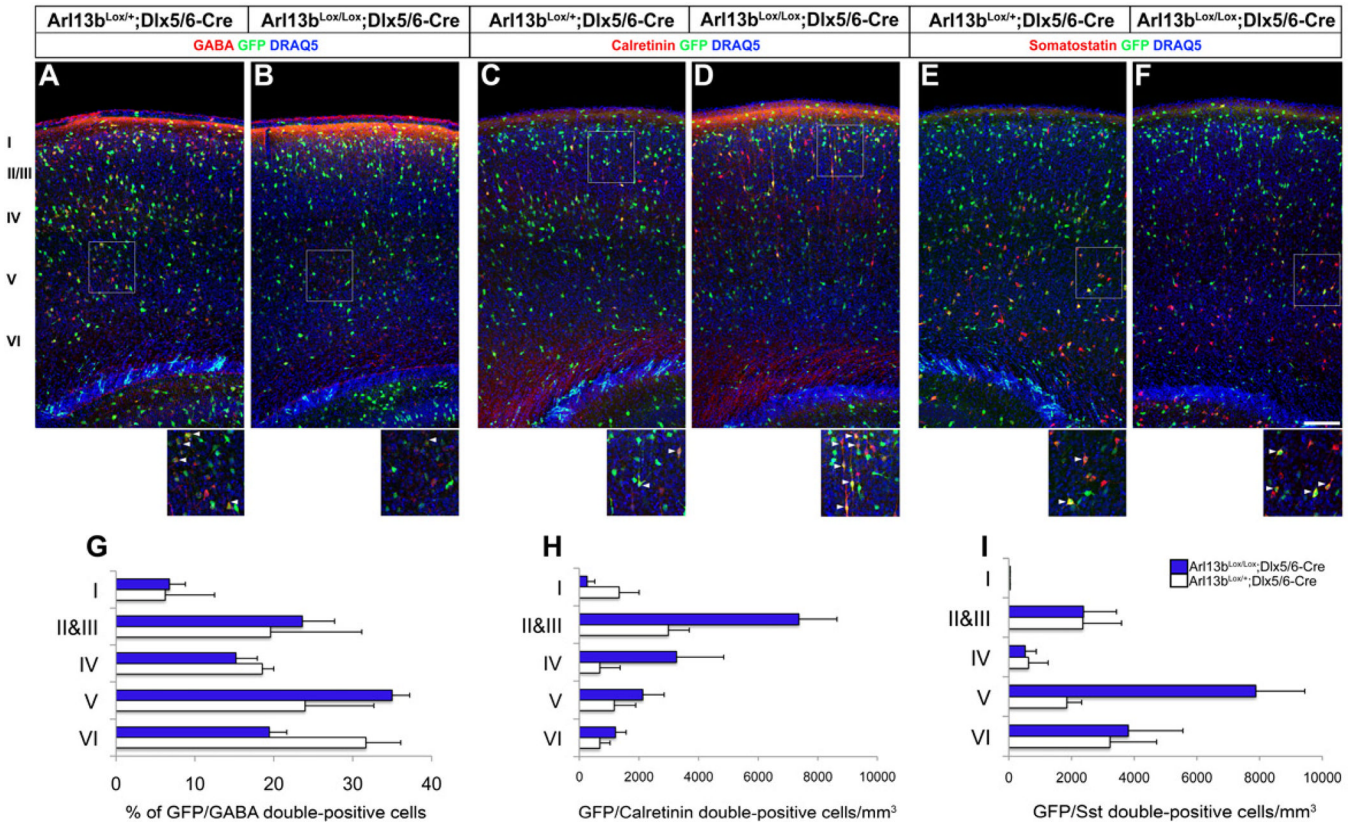

Figure 2. Interneuronal placement is disrupted after Arl13b deletion in interneurons

(A-F) P10 control Arl13b$^{Lox/+}$;Dlx5/6-CIE (A, C, E) and Arl13b$^{Lox/Lox}$;Dlx5/6-CIE (B, D, F) cortices were co-labeled with GFP (Cre^{+}) and GABA (A, B) calretinin (C, D) and somatostatin (E, F). Insets show higher magnification images of double-positive cells (arrowheads). (G-I) Quantification of changes in the distribution of double-positive cells across cortical layers. Sections were from somatosensory cortex and counterstained with DRAQ5 [blue]. Data shown are mean ± SEM; * indicates significant when compared with controls at $p<0.05$ (Student's t test). $p<0.05$ (Student's t test). Scale bar= 100μm.

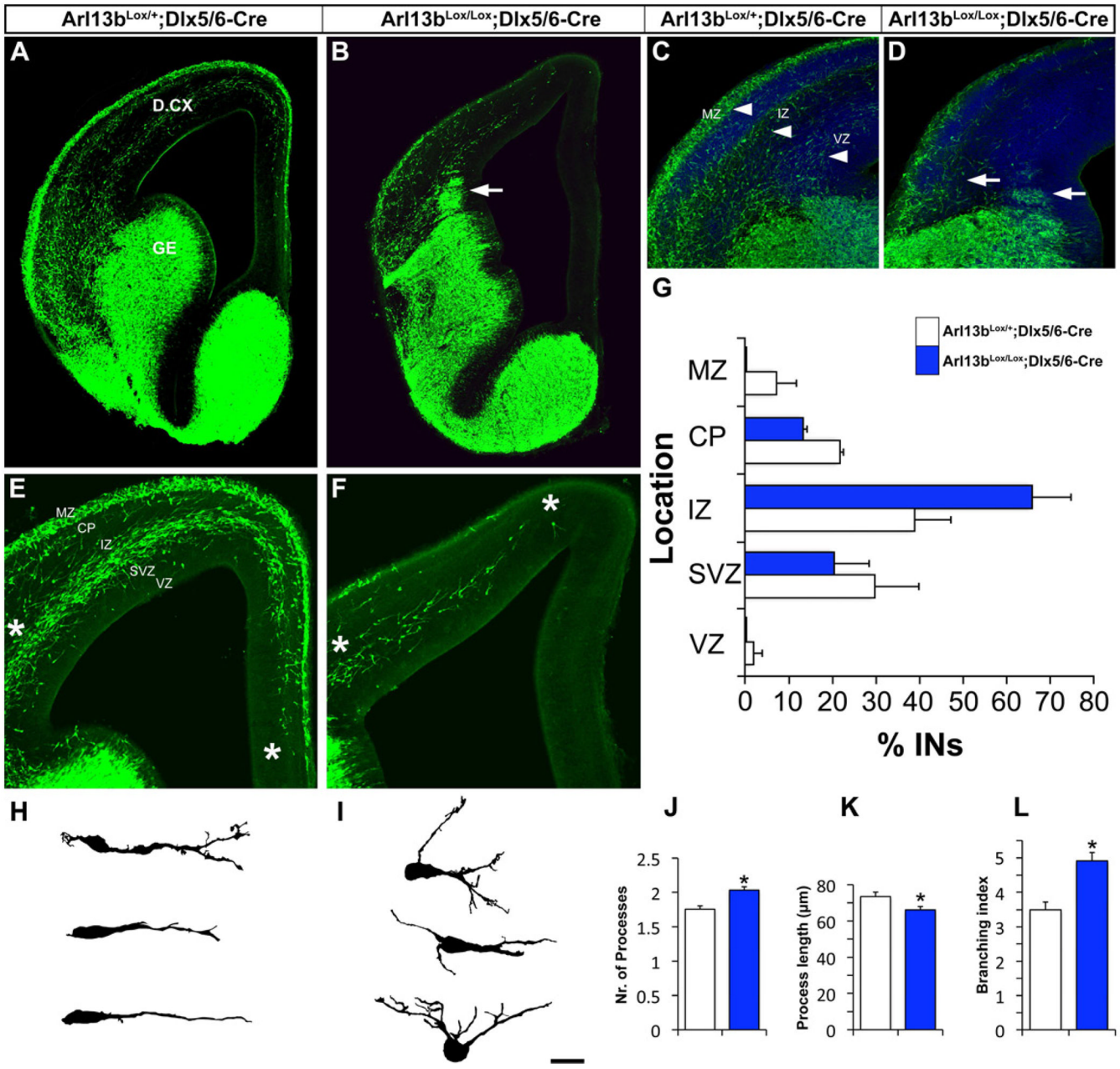

Figure 3. Arl13 deletion leads to interneuronal migration and branching defects

(A-B) GFP-labeled coronal hemisections show interneuron migration defects in Arl13b$^{Lox/Lox}$;Dlx5/6-CIE mutants, with clusters of cells stuck at the pallial-subpallial boundary (arrow, 5B). (C-D) Loss of characteristic interneuronal migratory streams in Arl13b$^{Lox/Lox}$;Dlx5/6-CIE cortex. Arrowheads in C indicate streams of migrating interneurons in the MZ, IZ and SVZ of control cortex. Arrows in D indicate disruptions in these streams in mutant cortex. (E-F) Higher magnification images of the control (E) and mutant (F) dorsal cortex illustrating disrupted extent and patterns of migration in mutants. Left asterisks mark pallial-subpallial boundary, right asterisks mark the migration front. (G) Disrupted migration results in altered distribution of interneurons (INs) across the cortical wall in Arl13b$^{Lox/Lox}$;Dlx5/6-CIE cortex, with a larger percentage of cells moving through the intermediate zone (IZ) and a corresponding loss of cells in other locations. The overall

number of interneurons was reduced in mutants, but mutants show a higher percentage of interneurons in the IZ than controls. (H, I) Camera lucida drawings of sample control (H) and mutant (I) interneurons in the dorsal cortex. (J-L) Quantification of branching defects in Arl13b-deficient interneurons. (J) Number of processes extending from cell soma. (K) Total process length (n=506 cells each from control and mutants). (L) Branching index (average number of branching events in a migrating interneuron per hour). Data shown are mean ± SEM; * indicates significant when compared with controls at $p<0.05$; ** indicates significant when compared with controls at $p<0.01$ (Student's t test). VZ-ventricular zone, SVZ-subventricular zone, IZ-intermediate zone, CP-cortical plate, GE-ganglionic eminence, D.CX-dorsal cortex. Scale bar= A-D, 675μm; E-F, 225μm; G-H, 100μm; J-K, 25μm.

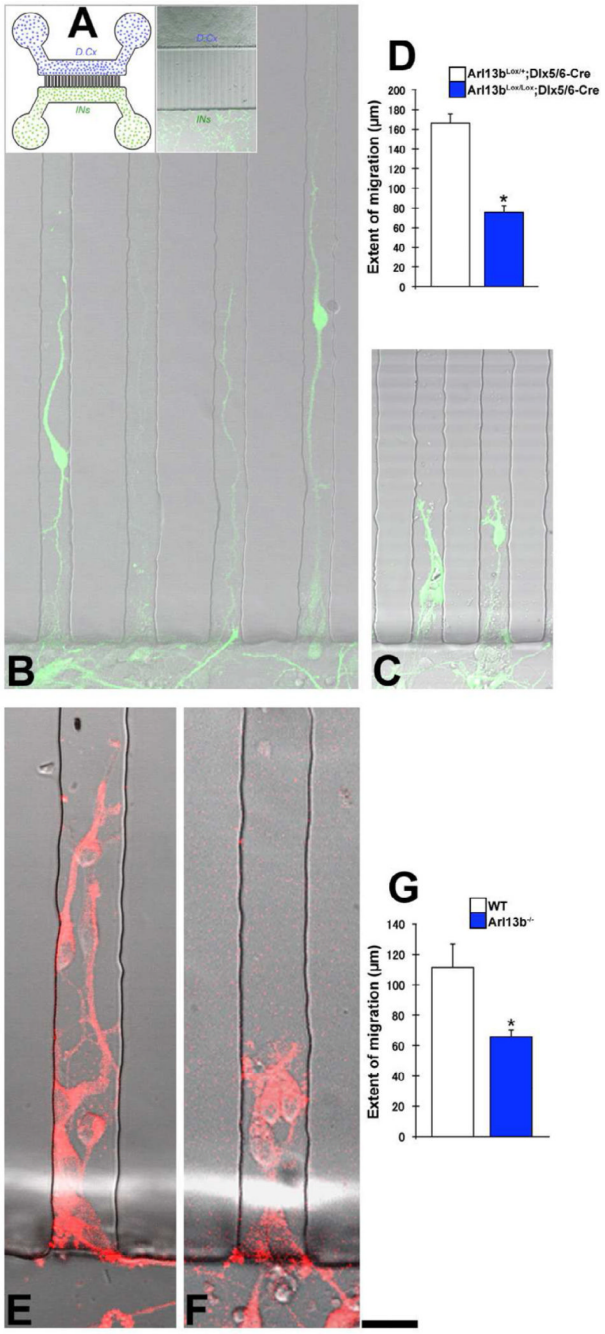

Figure 4. Arl13b is required for interneuron migration through a microgradient of endogenous guidance cues from dorsal cortex

(A) Left: Schematic of microfluidic chamber migration assay. Dissociated wild-type dorsal cortical cells (D. Cx, blue) are plated in one side of a chamber and dissociated interneurons from the GE of control (Arl13b$^{Lox/+}$; Dlx5/6-CIE or Arl13b$^{+/-}$) or mutant (Arl13b$^{Lox/Lox}$; Dlx5/6-CIE or Alr13b$^{-/-}$) cortex are plated in the other side. Right: Brightfield/fluorescent image of the assay soon after plating of neurons. Interneurons were exposed to a microfluidic gradient of cues released by dorsal cortical neurons. Interneurons migrate toward the dorsal cortical cells via microchannels (vertical lanes) separating the chambers. (B-G) Compared to control Arl13b$^{Lox/+}$ (B), GFP^{+} interneurons from Arl13b$^{Lox/Lox}$;

Dlx5/6-CIE brains (C) migrated significantly shorter distances (D). Similar defects in migration occurred in interneurons from Arl13b$^{-/-}$ brains (E-G). Interneurons from Arl13b$^{-/+}$(E) or Arl13b$^{-/-}$(F) brains were immunolabeled (red) with anti-GAD67 antibodies. Data shown are mean ± SEM; * indicates $p<0.01$ (Student's t test). Scale bar= B-C, 15μm; E-F, 30μm.

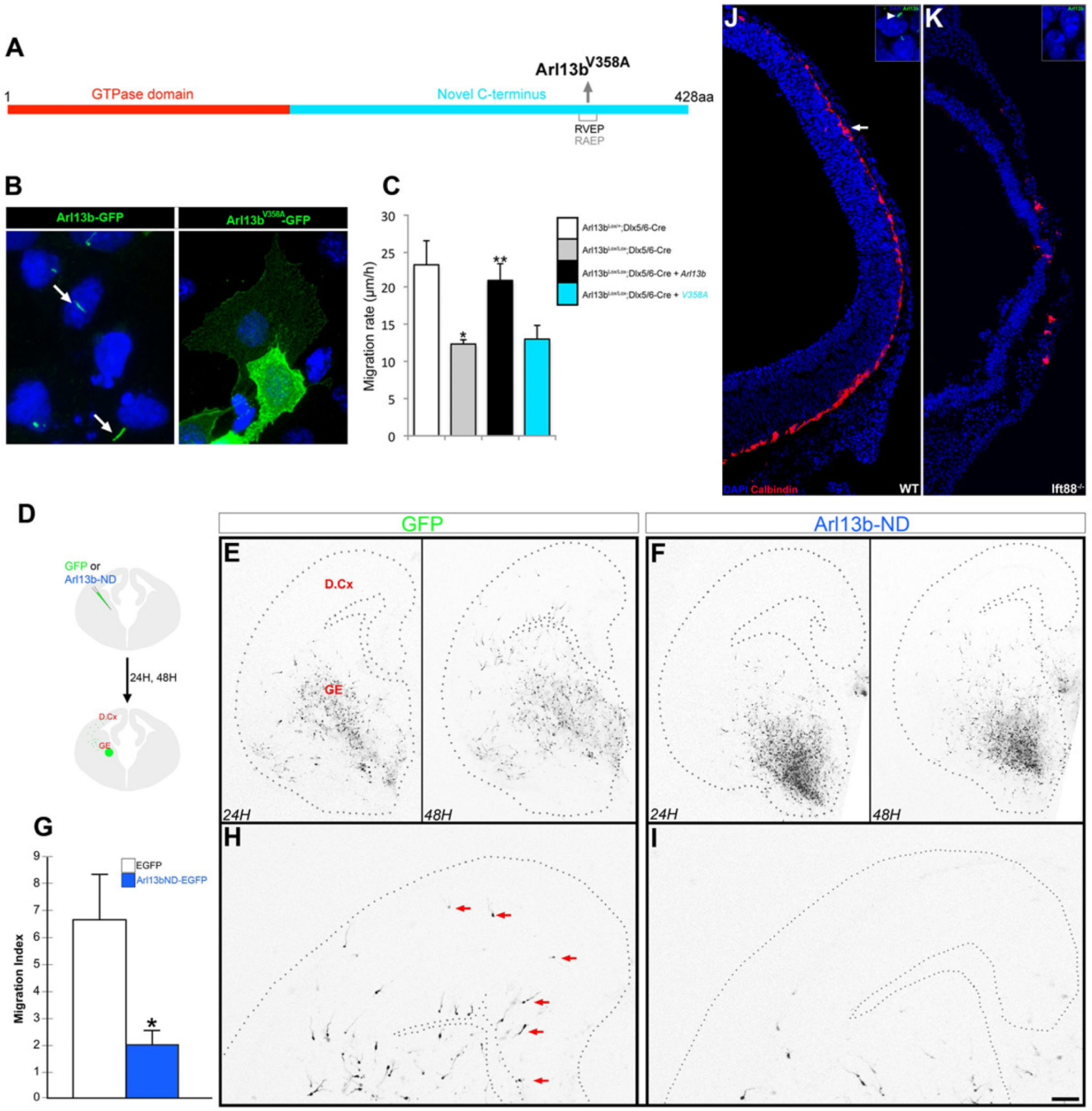

Figure 5. Ciliary function of Arl13b is critical for the regulation of interneuron migration

(A) Schematic of a non-ciliary form Arl13b (Arl13b^{V358A}). (B) In ciliated IMCD3 cells transfected with control Arl13b-GFP and Arl13b^{V358A}-GFP constructs, Arl13b-GFP localizes to cilia (arrow), but Arl13b^{V358A}-GFP does not. Nuclei were counterstained with DAPI. (C) Expression of wild type Arl13b rescued the migratory defect in Arl13b deficient (Arl13b$^{Lox/Lox}$; Dlx5/6-CIE) interneurons. In contrast, expression of Arl13b^{V358A} did not rescue the defect. Data shown are mean ± SEM (n=42 [Control: Arl13b$^{Lox/+}$; Dlx5/6-CIE], 79 [Arl13b deficient: Arl13b$^{Lox/Lox}$; Dlx5/6-CIE], 104 [Arl13b$^{Lox/Lox}$; Dlx5/6-CIE +Arl13b], 49 [Arl13b$^{Lox/Lox}$; Dlx5/6-CIE+Arl13b^{V358A}]); * indicates significant when compared with controls at $p<0.001$; ** indicates significant when compared with Arl13b

mutant at $p<0.001$ (Student's t test). (D-H) Dominant negative N-terminal domain (Arl13b-ND) of Arl13b disrupts selective targeting of Arl13b to primary cilia and inhibits interneuronal migration. (D) Cartoon of experimental protocol. Arl13b-ND/GFP or GFP DNA was focally electroporated into the MGE of E14.5 coronal slices. Images of GFP^+ interneuronal migration into dorsal cortex were acquired at 24 and 48 hours. (E-H) Interneurons expressing GFP alone leave the MGE at 24 h (E, left panel) and migrate into the dorsal cortex by 48 h (E, right panel, and higher magnification image of dorsal cortex in H). Interneurons co-expressing Arl13b-ND mostly remain in the GE at 24 h (F, left panel) and show less migration into dorsal cortex at 48 h (F, right panel, and higher magnification image in I). Compared to control (arrows, H), fewer GFP^+ interneurons are seen in the dorsal cortex in Arl13b-ND slices (I). (G) Quantification of changes in the extent of interneuronal migration. Migration index indicates the number of cells migrating greater than 350 μm past the GE-dorsal cortex boundary. Data shown are mean ± SEM (n=36 slices/group); * $p<0.05$ (Student's t test). GE, ganglionic eminence; D.Cx, dorsal cortex. (J-K) Disrupted interneuron migration in $Ift88^{-/-}$ brains. (I) $Calbindin^+$ interneurons (red, arrow) migrate from the ganglionic eminence into the dorsal cortex. This migration is severely disrupted in $Ift88^{-/-}$ brain (K). Insets (I, K) show the presence and absence of $Arl13b^+$ cilia in wild type and mutant brains, respectively. Sections were counterstained with DAPI or DRAQ5 (blue). Scale bar= B-C, 34 μm; E-F, 400 μm; H-I, 175 μm; J-K, 180 μm.

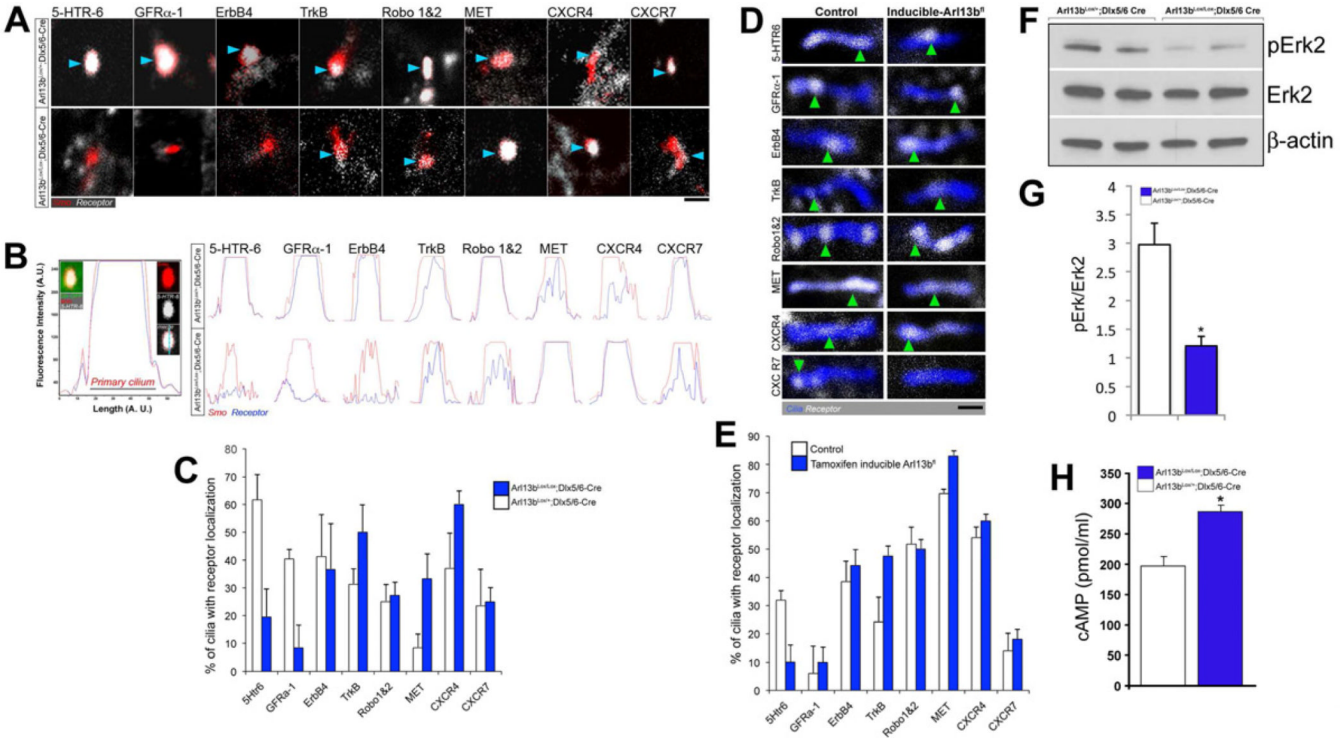

Figure 6. Changes in the primary cilia localization of interneuronal migration related guidance cue receptors and second messenger activity in Arl13 deficient interneurons

(A) Primary cilia (red) of control Arl13b$^{Lox/+}$; Dlx5/6-CIE (top) and mutant Arl13b$^{Lox/Lox}$; Dlx5/6-CIE (bottom) interneurons were fluorescently labeled with Smoothened-tdTomato (red) and co-labeled with a panel of eight different antibodies against known interneuron migration cue receptors (white). Arrowheads point to cilia/receptor co-localization. These images depict the range of localization patterns observed for all receptors, none were restricted to a single part of the cilium (B) Fluorescent intensity (FI) line scans through Smo^{+} primary cilia in interneurons indicates the level of co-localization. Overlay of the red (Smo^{+} cilia) and blue (receptor labeling) FI measurement peaks indicates co-localization. The left panel in B illustrates 5-HTR-6 FI peaks in detail; FI peaks for other receptors in controls and mutants are shown at right. (C) Percent of control and mutant interneuronal cilia with receptor co-localization. Data shown are mean ± SEM (n=4). (D) Primary cilia (blue) in wild type and inducibly deleted, Arl13 deficient MEFs were also co-labeled with receptor (white) antibodies. Acetylated tubulin or ACIII antibodies were used to immunolabel cilia in MEFs. Arrowheads point to cilia/receptor co-localization. Arl13b deletion altered the percentage of MEF cilia containing these receptors (E). Data shown are mean ± SEM (n=3). (F) Erk1/2 phosphorylation decreases in Arl13b mutant interneurons. (G) Quantification of the decrease in Erk1/2 phosphorylation. Densitometric measurements of phosho-Erk (pERK) bands were normalized to Erk2 expression. (H) cAMP levels increase in Arl13b$^{Lox/Lox}$; Dlx5/6-CIE GE interneurons. Data shown are mean ± SEM; * indicates $p<0.01$ (Student's t test). Scale bar = 2.4 μm (A); 1.25 μm (D).

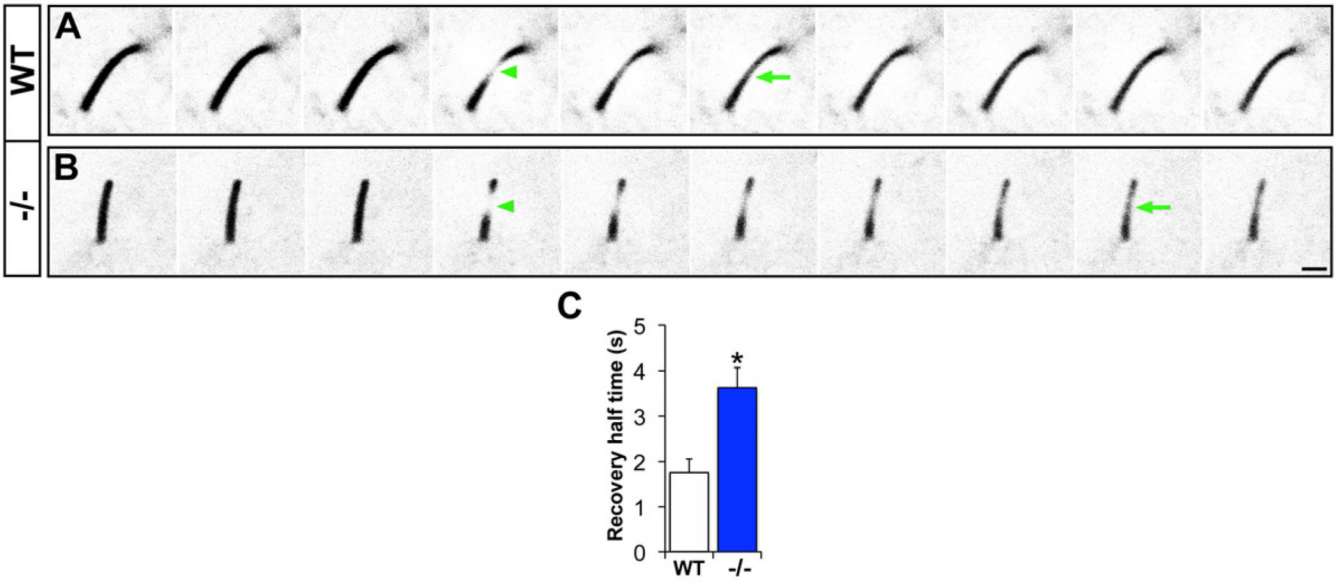

Figure 7. Interneuronal migration guidance cue receptor transport is defective in Arl13b-deficient primary cilia

Wild-type and Arl13b$^{-/-}$ cells express 5-Htr6-GFP in primary cilia. A subregion of the primary cilium was photobleached (green arrowhead, A-B) and fluorescence recovery over time was monitored. Compared to fluorescence recovery in control cilia (A, arrow), recovery was significantly delayed in mutant cilia (B, arrow). (C) Quantification of the recovery half-time. Data shown are mean ± SEM (n=14 [WT], 21 [−/−]); ** indicates $p<0.01$ (Student's t test). Time interval between each panel is 1.125 seconds. Scale bar = 1μm.

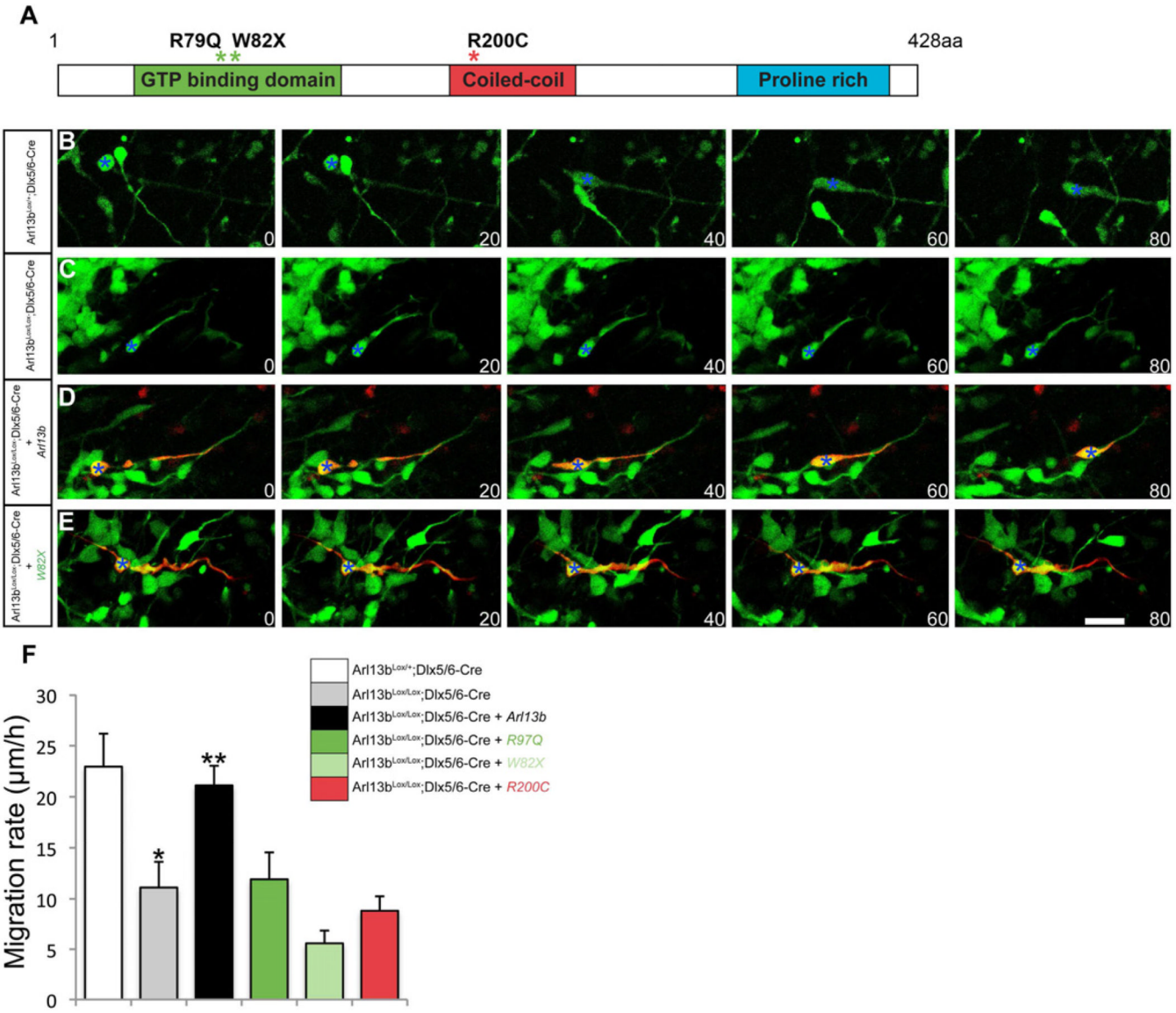

Figure 8. Expression of mutated human Arl13b allele disrupts interneuron migration

(A) Pathogenic ARL13B mutations R79Q, W82X, R200C cause Joubert syndrome. (B-E) Panels from timelapse imaging of control ($Arl13b^{Lox/+}$; Dlx5/6-CIE; B), Arl13b deficient interneurons ($Arl13b^{Lox/Lox}$; Dlx5/6-CIE; C), and Arl13b deficient interneurons expressing either WT (D) or W82X (E) human Arl13b (red). sterisks (B-E) indicate cell soma of migrating interneurons. Time elapsed between panels is in minutes. (F) Reduction in the rate of migration in Arl13b deficient interneurons is rescued by expression of human Arl13b. R79Q, W82X and R200C mutant Arl13b constructs fail to rescue, suggesting that these mutations impair interneuron migration. Data shown are mean ± SEM (n=40 cells for each condition) * indicates $p<0.001$ compared with control; ** indicates $p<0.001$ when compared with Arl13b deficient cells (Student's t test). Scale bar=75μm.